Analysis of Dielectric Guiding Structures by the Iterative Eigenfunction Expansion Method

TOMASZ F. JABŁOŃSKI AND MACIEJ J. SOWIŃSKI

Abstract—**Numerical results demonstrating capabilities of a recently developed method for determining guided modes of dielectric waveguides are presented. Apart from accuracy tests for the single-core waveguides, examples of the wavelength-selective coupler, the directional coupler with an adhesive layer, and of the side-pit structure are briefly analyzed. The theoretical background of the iterative eigenfunction expansion method (IEEM) and a comprehensive description of the numerical algorithm are also given. As it is efficient, highly accurate, and versatile, the IEEM proved to be useful in the analysis of various dielectric guiding structures.**

I. Introduction

IN ORDER TO achieve certain desirable properties of a given dielectric waveguide many different shapes, profiles, and core configurations have been used or proposed for use at optical and millimeter-wave frequencies. When the rigorous vectorial description of the guided modes is indispensable and the permittivity of the waveguide cross section, $\epsilon = \epsilon(x_1, x_2)$, is a function without radial symmetry, there are only a few reasonable methods which can be used for computation. Among them, in the optical wavelengths, varieties of the finite element method [1]–[4] are most commonly used. They differ mainly in the conditions imposed on the far-field pattern of the guided mode. For the millimeter-wave structures the finite difference method is preferred by the authors [5], [6]. Apart from these two dominant methods the following ones are also available: the domain integral equation method [7], the alteration formulas method [8], and the effective cross section method [9].

In each of these methods one stage requires considerable computational effort, viz. that in which the waveguide geometry is coded into the set of algebraic equations or into the solution of the auxiliary structure. Admittedly, due to extensive information encoded in the matrix coefficients, we can obtain all the guided modes of a given structure, but very often we are interested in only a few of them.

Manuscript received October 28, 1987; revised April 29, 1988. This research was completed while M. J. Sowiński was a Research Fellow at the Laboratory of Electromagnetic Research, Delft University of Technology, Delft, The Netherlands.

The authors are with the Department of Electromagnetic Wave Theory, Institute of Fundamental Technological Research, Polish Academy of Sciences, 00-049 Warsaw, Poland.

IEEE Log Number 8823263.

In this paper some capabilities of a new method for solving boundary eigenproblems are presented. Efficiency and potentialities for finding the guided modes of a wide class of dielectric waveguides make the method, in our opinion, complementary to those mentioned above. Here, in the method called the iterative eigenfunction expansion method (IEEM) [10], each eigensolution of the problem is sought for in the iterative process as an expansion in the basis consisting of the eigenfunctions of some known operator. Roughly speaking, the operator which corresponds to the given eigenproblem is decomposed into two parts. The first (main) part yields the basis for the expansion of the solution and the second is considered as the perturbation of the first one. In the case of the waveguide problem this (not necessarily small) perturbation represents nonhomogeneity of the refractive index in the core's cross section with respect to the homogeneous neighborhood represented by the first main part of the decomposition. Such an approach allows the computation of modes of a wide class of dielectric waveguides by a single numerical realization of the method. Moreover, "algebraization" of the problem is avoided and thus the first guided modes of more complicated dielectric structures can be analyzed without any essential limitation.

II. Theory

A. General Description of the IEEM

Let the boundary eigenproblem be given as follows:

$$(\mathbb{T} - \beta^2)u = 0 \tag{1}$$

represented by the operator $\mathbb{T}$ acting in a suitably chosen Hilbert space $\mathscr{H}$. In order to apply the IEEM to solve (1) it is necessary to decompose $\mathbb{T}$ into two parts:

$$\mathbb{T} = \mathbb{L} - \mathbb{F} \tag{2}$$

such that $\mathbb{L}$ has a known discrete spectrum $\sigma(\mathbb{L}) = \{(\lambda_m)_{m=1}^{\infty}\}$ with eigenfunctions $(e_m)_{m=1}^{\infty}$ given by

$$(\mathbb{L} - \lambda_m)e_m = 0, \qquad m = 1, 2, 3, \cdots. \tag{3}$$

These eigenfunctions should form the basis in $\mathscr{H}$ (best of all an orthogonal one). In the decomposition (2) it is desirable that the (unbounded) operator $\mathbb{F}$ be relatively

0018-9480/89/0100-0063$01.00

compact with respect to $\mathbb{L}$, meaning that

$$\mathbb{F}(\mathbb{L}-\rho)^{-1} \tag{4}$$

is the compact operator for all $\rho \notin \sigma(\mathbb{L})$.

If the above conditions are satisfied the solutions u, β^2 of (1) can be obtained by the iterative process called the iterative eigenfunction expansion method (IEEM). Keeping in mind that (1) is equivalent to

$$(\mathbb{L}-\beta^2)u = \mathbb{F}u \tag{5}$$

the loop of the IEEM consists in the following:

a) To find u_n—the nth approximation to u—we solve the nonhomogeneous equation for ψ_n (with u_{n-1} and β_{n-1} known from the previous step):

$$(\mathbb{L}-\beta_{n-1}^2)\psi_n = \mathbb{F}u_{n-1}. \tag{6}$$

The solution of (6) always exists, since $\beta_{n-1}^2 \notin \sigma(\mathbb{L})$. Using $\mathbb{L}$-eigenfunctions expansion we obtain ψ_n in the form

$$\psi_n = \sum_m C_m^n e_m \tag{7}$$

with coefficients C_m^n in the orthonormal basis $(e_m)_{m=1}^{\infty}$ given as

$$C_m^n = \frac{(\mathbb{F}u_{n-1}, e_m)_{\mathscr{H}}}{\lambda_m - \beta_{n-1}^2}. \tag{8}$$

Here $(\cdot,\cdot)_{\mathscr{H}}$ denotes the scalar product in $\mathscr{H}$. We finally put

$$u_n = \|\psi_n\|_{\mathscr{H}}^{-1}\cdot\psi_n = \sum_m D_m^n e_m \tag{9}$$

where the norm of ψ_n is found from the Parseval equality:

$$\|\psi_n\|_{\mathscr{H}}^2 = \sum_m |C_m^n|^2 \tag{10}$$

and the normalized coefficients of u_n are

$$D_m^n = \|\psi_n\|_{\mathscr{H}}^{-1}\cdot C_m^n. \tag{11}$$

b) In order to obtain β_n, the new approximation to β, we substitute u_n into the following formula, which follows from (1), (9), (2), and (6):

$$\begin{aligned}\beta_n^2 &= (\mathbb{T}u_n, u_n)_{\mathscr{H}} \\ &= \beta_{n-1}^2 + \left(\mathbb{F}\left(\|\psi_n\|_{\mathscr{H}}^{-1}\cdot u_{n-1} - u_n\right), u_n\right)_{\mathscr{H}}.\end{aligned} \tag{12}$$

Equation (12) has the computationally convenient form

$$\begin{aligned}\beta_n^2 &= \beta_{n-1}^2 \\ &\quad + \sum_m \left\{\left(\lambda_m - \beta_{n-1}^2\right)|D_m^n|^2 - \overline{D_m^n}\cdot(\mathbb{F}u_n, e_m)_{\mathscr{H}}\right\}.\end{aligned} \tag{13}$$

$\beta_0^2 \notin \sigma(\mathbb{L})$ and u_0 such that $\mathbb{F}u_0 \not\equiv 0$ are the necessary conditions for the initial approximation.

B. Application of the IEEM to the Dielectric Waveguide Problem

The IEEM has been applied to solve the propagation eigenproblem for guided modes of the dielectric waveguide which is homogeneous along the direction of propagation and possesses arbitrary cross section. Arbitrariness has to do with the shape and number of cores as well as with their refractive index profiles.

The unknown transversal magnetic vector field $H_\perp$ of the guided mode and its propagation constant β satisfy the following boundary eigenproblem (factor $e^{\imath(\beta z-\omega t)}$ is suppressed throughout):

$$\begin{aligned}&\nabla_\perp^2 H_\perp + k^2\epsilon(x)H_\perp \\ &\qquad + \epsilon^{-1}(x)\{\nabla_\perp\epsilon(x)\times(\nabla_\perp\times H_\perp)\} - \beta^2 H_\perp = 0 \\ &\left(H_\perp^+ - H_\perp^-\right)\big|_{\partial P} = 0 \qquad \left(\nabla_\perp\cdot H_\perp^+ - \nabla_\perp\cdot H_\perp^-\right)\big|_{\partial P} = 0 \\ &\left\{(\epsilon^+)^{-1}(\nabla_\perp\times H_\perp^+) - (\epsilon^-)^{-1}(\nabla_\perp\times H_\perp^-)\right\}\big|_{\partial P} = 0 \\ &\qquad H_\perp \text{ vanishes at infinity.}\end{aligned} \tag{14a}$$

Here P is the cross section of the circular cladding of the waveguide, $x \in \mathbb{R}^2 \supset P$; the superscripts + and − denote the interior and the exterior of P, respectively; $k^2 = \omega^2\mu\epsilon_0$, where μ is the permeability of the waveguide medium; and ϵ_0 is the permittivity of the vacuum. The relative (complex) permittivity function $\epsilon(x)$: $\mathbb{R}^2 \to \mathbb{C}$ is assumed to satisfy the following conditions:

$$\begin{aligned}&\epsilon(x) = \begin{cases}\epsilon_P + \epsilon_s(x) & x \in P \\ 1 & x \in \mathbb{R}^2 - P\end{cases} \\ &\epsilon_P = \text{const} \qquad \epsilon_s(x) = (\epsilon_{\max} - \epsilon_P)\cdot s(x) \in H_0^2(S) \\ &S = \bigcup_{i=1}^{J} S_i \subset P \qquad \operatorname{diam} S \ll \operatorname{diam} P = 2\cdot r_P\end{aligned} \tag{14b}$$

where S is an arbitrarily shaped cross section of the cores and the normalized refractive index profile of the cores $s(x)$ belongs to the local Sobolev space $H_0^2(S)$—the completion of the space of smooth functions with compact support $C_0^\infty(S)$ in the norm [11]:

$$\|\cdot\|_m^2 = \sum_{|\alpha|\le m} \|D^\alpha\cdot\|_{L^2(S)}^2, \qquad \alpha = (\alpha_1, \alpha_2).$$

This means that the profile function $s(x)$ vanishes outside the core region S which is embedded into the relatively large homogeneous cladding P with $\epsilon_P = \text{const}$. Moreover, $s(x)$ is square integrable over S together with its derivatives (in the distribution sense) up to the second order. The above assumptions are quite general and a wide class of dielectric structures, including single-core and multicore and step-index and gradient-index waveguides, can be represented by the function $\epsilon(x)$ defined in (14b).

The operator $\mathbb{T}$ corresponding to the boundary problem ((14a) and (14b)) is defined in the Hilbert space $\mathscr{H}$ of square integrable complex-valued vector functions defined on P:

$$\mathscr{H} := L^2(P)\otimes\mathbb{C}^2 \tag{15}$$

with the scalar product

$$\begin{aligned}(u, v)_{\mathscr{H}} &:= \int_P \sum_{i=1}^{2} u_i(x)\overline{v_i(x)}\,dx = \sum_{i=1}^{2}(u_i, v_i)_{L^2(P)}, \\ &u, v \in \mathscr{H}; \quad u = [u_1, u_2]; \quad v = [v_1, v_2].\end{aligned} \tag{16}$$

The unbounded operator $\mathbb{T}$ has the form

$$\mathbb{T}u := \nabla_\perp^2 u + k^2 \epsilon_P u + k^2 \epsilon_s(x) u + \epsilon^{-1}(x) \cdot \{\nabla_\perp \epsilon_s(x) \times (\nabla_\perp \times u)\} \quad (17a)$$

with domain $D(\mathbb{T})$ chosen as

$$D(\mathbb{T}) := \{ f \in H_0^1(P): f \in C^2 \text{ down to } \partial P, f|_{\partial P} = 0 \} \otimes \mathbb{C}^2. \quad (17b)$$

Each component of $u \in D(\mathbb{T})$ belongs to the domain of the so-called Dirichlet Laplacian [11] acting in $L^2(P)$ and thus is equal to zero at the edge of the circle P. Such a choice of $D(\mathbb{T})$ provides a good correspondence of the operator $\mathbb{T}$ to the problem (14), since it is well known that guided modes —the eigensolutions of (14)—decay exponentially outside the cores region.

It has been proved in [12] that the operator $\mathbb{T}$ defined by (17a) and (17b) can be decomposed in such a way that the IEEM applicability conditions (2), (3), and (4) are satisfied. Indeed, in the case considered,

$$\mathbb{L} := \nabla_\perp^2 + k^2 \epsilon_P \qquad D(\mathbb{L}) = D(\mathbb{T}) \quad (18)$$

is the Dirichlet Laplacian on the circle P. It is well known that $\mathbb{L}$ is a self-adjoint operator with the following discrete spectrum:

$$\sigma(\mathbb{L}) = \{ \lambda_m \in \mathbb{R}: \lambda_m = k^2 \epsilon_P - p_m^2 \} \quad (19)$$

where $m = (\nu, \mu)$, $\nu = 0, 1, 2, \cdots$, $\mu = 1, 2, 3, \cdots$, and $p_{\nu\mu}$ are such that $J_\nu(p_{\nu\mu} \cdot r_P) = 0$, J_ν being the Bessel function of the first kind of order ν. The eigenfunctions e_m of $\mathbb{L}$ form the orthonormal basis in $\mathscr{H}$ and $e_{\nu\mu} = [e_{\nu\mu}^1, e_{\nu\mu}^2]$ are such that

$$e_{\nu\mu}^i = e_{\nu\mu}^i(r, \phi) = B_{\nu\mu}^{-1} \cdot J_\nu(p_{\nu\mu} r) \cdot \begin{cases} \sin(\nu\phi) \\ \cos(\nu\phi) \end{cases} \qquad i = 1, 2 \quad (20)$$

where

$$B_{\nu\mu} = r_P \cdot J_{\nu+1}(p_{\nu\mu} \cdot r_P) \cdot \begin{cases} (\pi)^{1/2}, & \nu = 0 \\ (\pi/2)^{1/2}, & \nu > 0 \end{cases}. \quad (21)$$

The second part of the decomposition (2) is defined as

$$\mathbb{F}u := -k^2 \epsilon_s(x) u - \epsilon(x)^{-1} \cdot \{\nabla_\perp \epsilon_s(x) \times (\nabla_\perp \times u)\} \qquad D(\mathbb{F}) = D(\mathbb{T}). \quad (22)$$

It is worth noting that the choice of the operator $\mathbb{L}$ in the decomposition (2) of the operator $\mathbb{T}$ determines the basis which is next used in the iterative process. In the case considered, the Dirichlet Laplacian (18) on the circle P provides eigenfunctions (20) which can be easily computed, and for simplicity this choice has been made in the present paper. The other choices of $\mathbb{L}$ are also possible, provided the IEEM applicability conditions (3) and (4) are satisfied.

Operator $\mathbb{F}$ maps $D(\mathbb{T})$ into functions with support contained in the core region S and represents the guidance abilities of the considered structure. In general, $\mathbb{F}$ is not symmetric in $\mathscr{H}$. From the relative compactness (4) of $\mathbb{F}$ with respect to $\mathbb{L}$, useful information concerning certain features of $\mathbb{T}$ can be inferred. $\mathbb{T}$ possesses a discrete spectrum and its eigenfunctions form the proper basis in $\mathscr{H}$ (the Riesz basis—not necessarily the orthogonal one). Moreover, if $\mathbb{F}$ is symmetric, then $\mathbb{T}$ is self-adjoint (e.g., $\mathbb{F}$ is symmetric under the assumptions of weak guidance and the reality of the $\epsilon(x)$ function).

C. Numerical Algorithm

IEEM can be easily transformed into a simple and inexpensive numerical algorithm. The only noticeable task for a computer is to evaluate $\mathscr{H}$ scalar products in (8), which by virtue of (16) and (14b) reduce to integrals of the form

$$\int_S (\mathbb{F} H_\perp^n)^i \cdot e_m^i \, ds, \qquad i = 1, 2 \quad (23)$$

over the core region S only. Integration is carried out by the Gauss method with integration points located in the smallest sector, say $r_1 < r < r_2, \phi_1 < \phi < \phi_2$, containing the domain S of the cores. Values of the eigenfunctions e_m and of the profile function $\epsilon_s(x)$ together with their derivatives are only computed once in the integration points, before entering the main loop of the IEEM. This fact makes it possible to reduce the crucial steps of the loop, namely (8), (10), and (13), to simple summing up processes. It is worth noting that for a fixed circle P eigenfunctions e_m and eigenvalues λ_m are the same for all waveguide geometries. Moreover, alterations of geometry which do not affect the smallest sector containing S require only a new computation of the profile values. The above facts make the algorithm universal and essentially speed up the computations.

In spite of numerical differentiation under operator $\mathbb{F}$ being avoided, summing up the $\mathbb{F}H_\perp^n$ values in the integration points is the most time-consuming process in the iterative loop. It can be speeded up by ignoring the relatively small expansion coefficients of $H_\perp^n$, according to the desired accuracy of the final result. Expenses are further reduced when the waveguide cross section possesses some symmetries. In this case, for each given mode, $H_\perp^n$ and $\mathbb{F}H_\perp^n$ are orthogonal (in the (16) scalar product sense) to the whole particular subseries of the eigenfunctions e_m, and the vector fields $H_\perp^n$ possess symmetries which are easily foreseeable. For example, when $\epsilon_s(x)$ has rectangular symmetry one can make use of the S–A classification [13], in which the guided modes split into four orthogonal subgroups according to the kinds of symmetries possessed. Numerical expenses are then reduced by a factor of 16, while for guiding structures with one symmetry axis a reduction by a factor of four is obtained.

The IEEM most easily finds the fundamental mode of a given structure. Further modes can also be obtained, provided they are orthogonal (in the (16) scalar product sense) to the previously found ones. The choice of the initial approximation, that is, the field $H_\perp^0$ and the propagation

constant β_0, determines which mode will be actually obtained. In most cases the choice of $H_\perp^0$ is crucial because for arbitrary $\beta_0^2 \in [k^2\epsilon_P, k^2\epsilon_{\max}]$ $H_\perp^1$ mainly depends on $\mathbb{F}(H_\perp^0)$ and the proper quantity of β_1^2 is next determined by $H_\perp^1$ in the first iteration, however, close to the cutoff frequency, when $\|(\mathbb{L}-\beta^2)^{-1}\|_{\mathscr{H}}$ becomes large, it is suitable to put $\beta_0^2 = k^2\epsilon_P$.

It seems to us that the convergence of the IEEM follows from the $\mathbb{L}$ compactness of $\mathbb{F}$ in the decomposition (2). A rigorous analytical proof of this fact is not yet available, but the convergence has been successfully confirmed numerically and no counterexample has been ever obtained. The change of β_n in the successive iterations and deviation of $\|\psi_n\|_{\mathscr{H}}$ from unity were used as the convergence criteria.

III. Numerical Examples

In this section several numerical examples are presented to show some possibilities of the IEEM. All these examples have been computed by the single Fortran language program on the IBM-PC/XT computer. All the geometries of the guiding structures considered can be defined by an appropriate superposition of at most three refractive index profiles $s(p)$ with elliptical supports of the form

$$s(p) = \begin{cases} 1 - \left\{ \left(\dfrac{x - x_0}{b_x} \right)^2 + \left(\dfrac{y}{b_y} \right)^2 \right\}^{\alpha/2}, & p \in S \\ 0, & p \notin S \end{cases} \quad (24)$$

where $p = (x, y) \in \mathbb{R}^2$, $\alpha \in \mathbb{R}^+$, and S is an ellipse with semiaxes b_x, b_y and center $p_0 = (x_0, 0)$. Results are presented in terms of the following nondimensional parameters:

$$V = k \cdot b_x \cdot \sqrt{\epsilon_{\max} - \epsilon_P} \qquad \Delta = \frac{\epsilon_{\max} - \epsilon_P}{2\epsilon_P}$$

$$Z = \left(\frac{\beta^2}{k^2} - \epsilon_P \right) \cdot (\epsilon_{\max} - \epsilon_P)^{-1} \quad (25)$$

V and Z being, respectively, the normalized frequency and propagation constant. The notation of $HE_{mn}^y(HE_{mn}^x)$ designates the particular HE_{mn} mode for which the dominant magnetic field is directed in the $y(x)$ direction.

A. Accuracy Tests

Let us recall that the solution of (14a) and (14b) is obtained as an expansion in the basis of $\mathbb{L}$ eigenfunctions (cf. (20) and (21)). There are three parameters which can affect accuracy, namely N_ν = number of the Bessel functions series with different orders ν, N_μ = maximal μ in the given ν series, and r_P = radius of P taken for the computation. Let us call these parameters the ν number, the μ number, and the math-clad radius, respectively.

The first accuracy test with respect to the math-clad radius r_P confirmed the proper selection of the domain $D(\mathbb{T})$ of the operator $\mathbb{T}$ defined in (17a) and (17b). Normalized propagation constants Z of the HE_{11} mode of the circular waveguide with the parabolic profile and $\Delta = 0.625$ versus r_P are shown in Fig. 1 for different V values. It is gratifying to see that infinity starts from $r_P = 3$ for V above the monomode range. Larger r_P is only needed close to the cutoff. In most of these cases $r_P \leqslant 20$ is sufficient to obtain satisfactory results. For example Z of the TM_{01} mode of the considered structure computed by the IEEM for $V = 3.230$ with $r_P = 17$ equals $0.16 \cdot 10^{-4}$, and Z of the HE_{31} mode for $V = 6.1598$ with $r_P = 12$ equals $0.12 \cdot 10^{-6}$. The above-mentioned V values are reported in [14] as the normalized cutoff frequencies of the TM_{01} and HE_{31} modes, respectively. They are computed by the method specially devised for structures with circular symmetry and thus can serve as a good reference point. Full plots of the dispersion curves of the HE_{11} and HE_{21} modes computed by the IEEM turned out to be identical with the corresponding plots presented in [14].

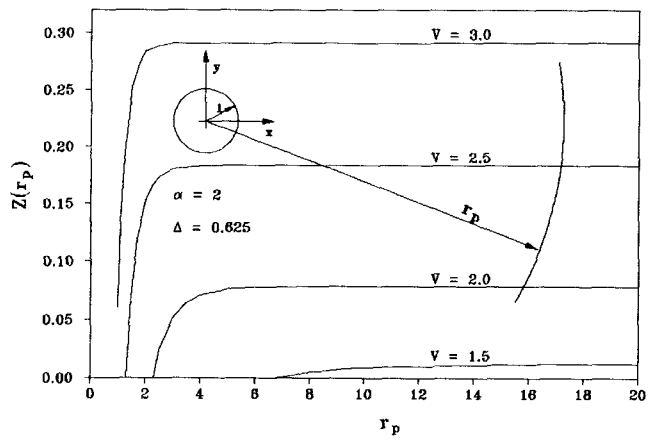

Fig. 1. Normalized propagation constants Z versus the math-clad radius r_P for the HE_{11} mode of the circular waveguide at different V values ($b_x = b_y = 1$, $\alpha = 2$, $\Delta = 0.625$).

Accuracy tests with respect to the μ number N_μ and the ν number N_ν give an idea of the extent of the expansion basis needed for the computation. In general, sufficient N_μ increases for greater r_P or for stronger radial variation of the field, while N_ν depends on the kind of symmetry of the structure and on the angular variation of the field.

The μ number test for the HE_{11} and HE_{21} modes of the circular waveguide with $\alpha = 200$ and $\Delta = 0.625$ is presented in Fig. 2. In this example $r_P = 5$ and $N_\nu = 2$ (there is no need for greater N_ν because of the circular symmetry of the guide). Dispersion curves a, b, c, d correspond to $N_\mu =$ 45, 7, 6, 5, respectively. The curve b of the HE_{11} mode (computed with $N_\mu \cdot N_\nu = 14$ eigenfunctions only) is indistinguishable from the curve a in the presented figure. Close agreement of the plotted curves in the usable part of monomode range is also noticeable.

The elliptical waveguide ($b_x = 1$, $b_y = 4$) with the parabolic profile and $\Delta = 0.625$ has been taken for the ν number test with fixed values $r_P = 8$ and $N_\mu = 45$. Dispersion curves of the HE_{11}^x and TM_{01} modes of this structure are plotted for different ν numbers in Fig. 3. Curves a, b, c correspond to $N_\nu = 13$, 2, 1, respectively. Again curve b of the HE_{11}^x mode is indistinguishable from curve a, which is believed to be exact.

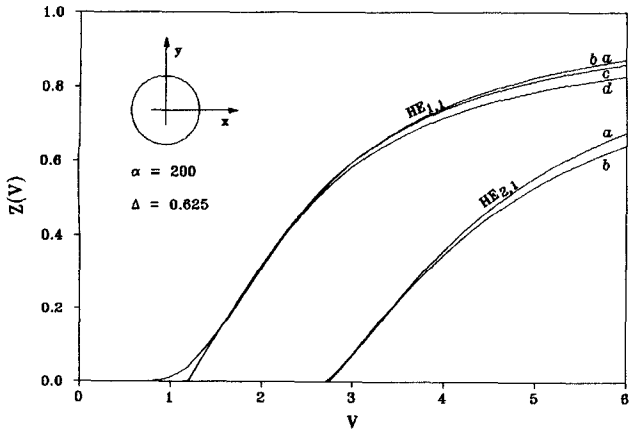

Fig. 2. Dispersion curves of the HE_{11} and HE_{21} modes of the circular waveguide for different μ numbers. Curves a, b, c, d correspond to $N_\mu = 45, 7, 6, 5$, respectively.

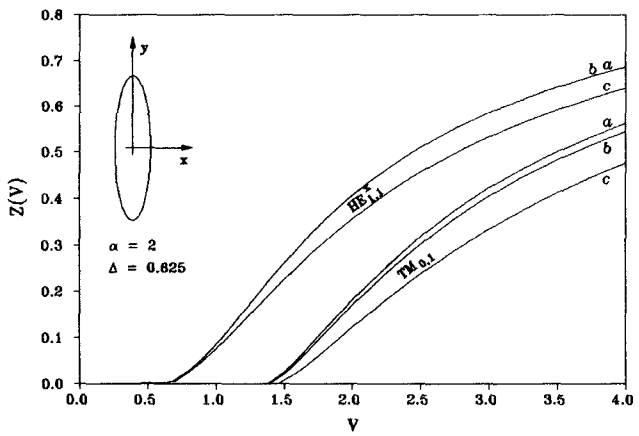

Fig. 3. Dispersion curves of the HE_{11}^x and TM_{01} modes of the elliptical waveguide ($b_x = 1$, $b_y = 4$) for different ν numbers. Curves a, b, c correspond to $N_\nu = 13, 2, 1$, respectively.

The above tests show that the IEEM is highly effective when such simple structures as single-core power profile waveguides with rectangular symmetry are to be analyzed. For example, in order to compute one point of the exact curve a in Fig. 3 with an accuracy of 10^{-4} the IEEM needs, on an average, five iterations. However, the IEEM is also applicable to much more complicated dielectric structures.

B. Wavelength Selective Coupler

Wavelength selective coupling can be obtained by making use of dissimilar dispersion characteristic of propagation constants in nonidentical single-mode fibers. Coupled modes analysis has been used in [15] to describe this phenomenon for step index circular fibers with nonidentical core radii and Δ parameters.

In the example presented, the asymmetry of the structure is enlarged by introducing ellipticity and a power profile index for one of the cores. The phenomenon is directly analyzed by evaluating $H_\perp$ of the fundamental antisymmetric A_1 mode of a double-core structure with no rectangular symmetry. Selectivity of the coupling can be judged by the rapidity of changes of the A_1 mode power

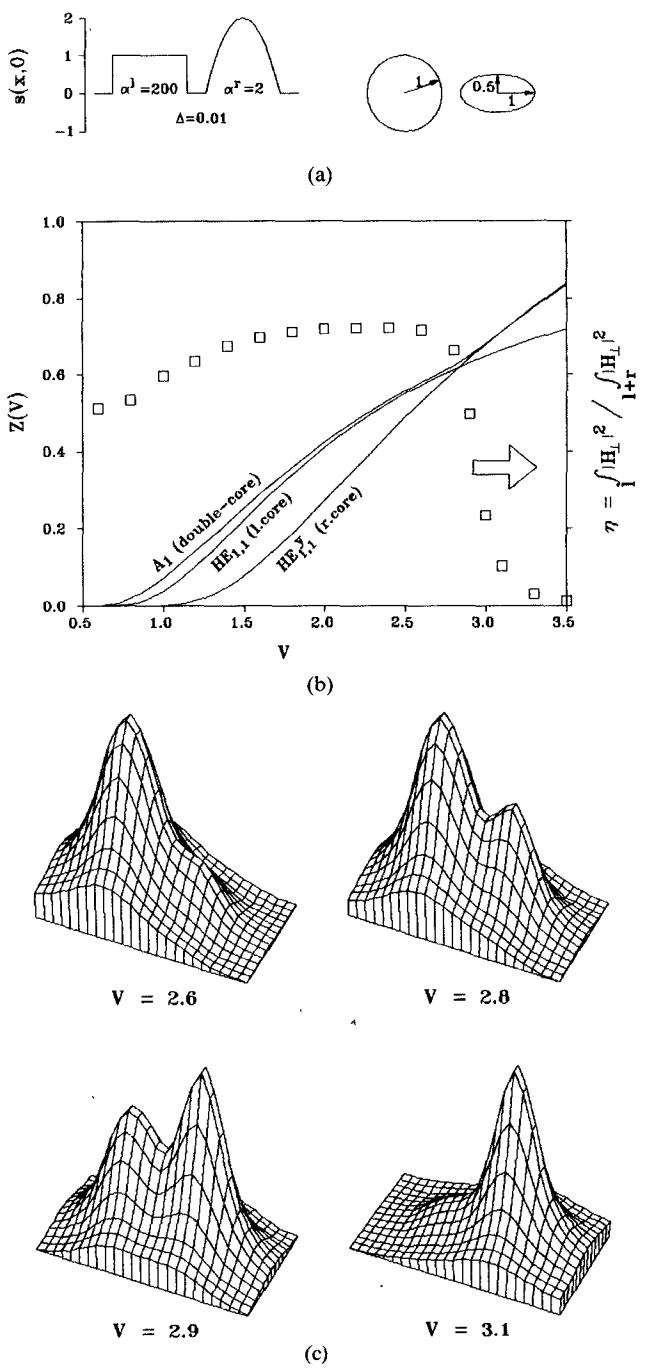

Fig. 4. Wavelength-selective coupler ($\alpha^r = 2$). (a) Specification of the structure. (b) Dispersion curves of fundamental modes of the double-core structure and of individual cores with V normalized to the left core. Squares denote the estimated fraction η of the A_1 mode power carried by the left core. (c) Plots of $|H_\perp|$ field of the A_1 mode in the neighborhood of the balanced power point visualizing selectivity of the coupling.

distribution over the cores in the neighborhood of the balanced power point. This point, which is, on the other hand, the cross point of the fundamental mode dispersion curves of the individual cores, corresponds to the maximal power transfer frequency of the coupler.

Two cases which differ in the right core profiles only ($\alpha^r = 2$ and $\alpha^r = 4$) are presented in Figs. 4 and 5. They show the excellent ability of the IEEM to pick up rapid

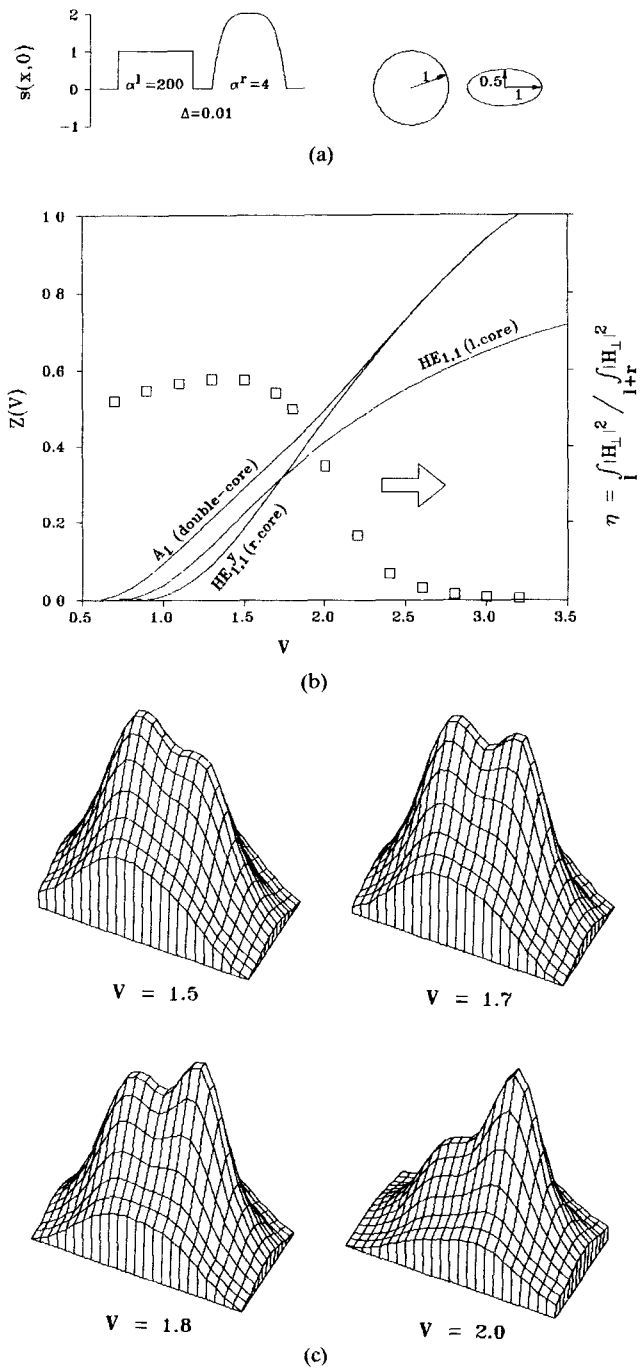

Fig. 5. Wavelength-selective coupler ($\alpha^r = 4$). Description the same as for Fig. 4.

alteration of the field in the neighborhood of the degeneracy point. They also demonstrate the high sensitivity of the phenomenon to changes in the fiber parameters.

C. Directional Coupler with an Adhesive Layer

In practically realizable directional couplers even a thin layer of the adhesive used for connecting the fibers can significantly affect the performance of a coupler. Perfect matching of the adhesive and clad refractive indexes is impossible because small clad–core index differences are used in practice.

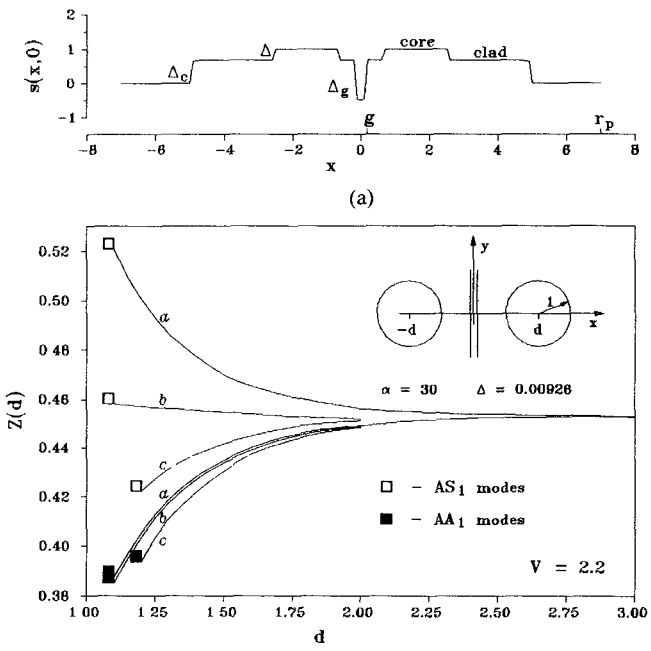

Fig. 6. Directional coupler with adhesive layer. (a) specification of the structure: $\Delta = (\epsilon_{\max} - \epsilon_{cl})/2\epsilon_{cl} = 0.00926$; $\Delta_g = (n_g^2 - \epsilon_{cl})/2\epsilon_{cl} = -3.59\Delta$; $\Delta_c = (\epsilon_{cl} - \epsilon_P)/2\epsilon_P = 0.02$; $2g$ = width of an adhesive layer. (b) Normalized propagation constants Z of the double-core AS_1 and AA_1 modes versus core separation for adhesive layers with different width $2g$: a – no adhesive-layer case; b – with $g = 0.1$; c – with $g = 0.2$.

In the example presented (Fig. 6), the performance of a coupler consisting of two circular cores and different adhesive layers with $n_g^2 < \epsilon_P$ is analyzed. The layer of width $2g$ is modeled by the narrow ellipse with $b_x = g$ and $b_y = 20$. The coupling effect can be easily analyzed with the aid of the S–A mode classification introduced in [13] for structures possessing rectangular symmetry. The HE_{11}^y mode energy transfer coefficient τ can be estimated from the total phase shift $\Delta\phi$ between the double-core AS_1 and AA_1 modes (the first modes in the antisymmetric–symmetric and antisymmetric–antisymmetric subgroups) which causes the coupling effect, that is,

$$\tau = 0.5 \cdot (1 - \cos \Delta\phi) \tag{26}$$

where $\Delta\phi$ can be found (via [13, formula (20)]) from the Z values of these modes for each different core separation. Three pairs of $Z(d)$ plots for fixed $V = 2.2$ are presented in Fig. 6(b). Cases a, b, c correspond to $\Delta_g = 0$, $\Delta_g = -3.59\Delta$ and $g = 0.1$, and $\Delta_g = 3.59\Delta$ and $g = 0.2$, respectively. Substantial damping of the coupling for thicker adhesive layers is evident from the figure.

To give a qualitative example, let us consider the symmetric directional coupler made from two bent silica-glass fibers with $\Delta = 0.00926$, radius of fiber curvature $R = 250$ mm, and minimum core separation $s = 1.9$ μm working at $\lambda = 1.3$ μm. For the adhesive with $n_g = 1.42$, the energy transfer coefficient τ, which equals 1 for the no-adhesive-layer case a, decreases to $\tau = 0.68$ in the case of b and to $\tau = 0.25$ in the case of c. When Δ is reduced to $\Delta = 0.00023$ then Δ_g corresponding to the same adhesive increases to

$\Delta_g = -14.36\Delta$ and the computation carried out has shown that τ can never exceed the value $3 \cdot 10^{-3}$ in this case. In conclusion, the adhesive with the refractive index significantly smaller than the clad index produces a deterioration of the coupling effect and should not be used in combination with fibers possessing a small core–cladding index difference.

D. Side Pit Structure

Degeneracy of the HE_{11} mode of a circular fiber can be eliminated by introducing two pits in the refractive index profile, one on each side of the core. The resulting modal birefringence ΔB between the HE_{11}^x and HE_{11}^y modes, defined as

$$\Delta B = (\beta_x - \beta_y)/\beta_x \tag{27}$$

serves then as a valuable measure of the effectiveness of the side pits. Moreover, when the profile function $s(p)$ of the structure satisfies the following condition [3]:

$$I_s := \int_S s(p)\, dp < 0 \tag{28}$$

then both the HE_{11} modes have different positive cutoff frequencies. A structure which approximates the elliptical core with two side pits and satisfies (28) has been analyzed in [3] with respect to the depth of the pits.

In Fig. 7 a canonical example of the side pit structure with a circular core of height equal to the depth of the pits is presented. Cases a, b, and c correspond to the conditions $I_s > 0$, $I_s = 0$, and $I_s < 0$, respectively. A remarkable increase of the fundamental mode birefringence ΔB can be observed for case c, for which the minimal beat length reaches the value of 2.4 mm (for $\lambda = 0.57\,\mu$m and $n = 1.47$).

E. Miscellaneous Remarks

Case c of the example discussed above in subsection D (with $I_s < 0$) is of special interest because it shows the behavior of the IEEM for the case when no eigensolution with $\beta^2 > k^2\epsilon_P (Z > 0)$ exists for a small enough positive V. The method converges then to the eigensolutions of the operator $\mathbb{T}$ which do not correspond to the modes guided in the core of the structure. The rate of convergence is then poor because all the eigenvalues of $\mathbb{T}$ are interspersed within the discrete spectrum of operator $\mathbb{L}$. In case c of the above example, this tendency appeared even above the cutoff (precisely at (V, Z) points equal to (1.6, 0.1028) for the HE_{11}^x mode and (1.7, 0.1326) for the HE_{11}^y mode).

This trouble can be overcome by "lifting up" the whole profile of the structure together with its sufficiently large circular neighborhood (corresponding to the physical cladding) and by including this neighborhood in the profile function $s(p)$. Such a regularization makes I_s positive and restores efficient convergence of the IEEM to the physically interpretable eigensolutions. However, each iteration consumes more time because of the increase in the number of integration points. The lifting up procedure has been successfully applied to the analysis of deep adhesive layers

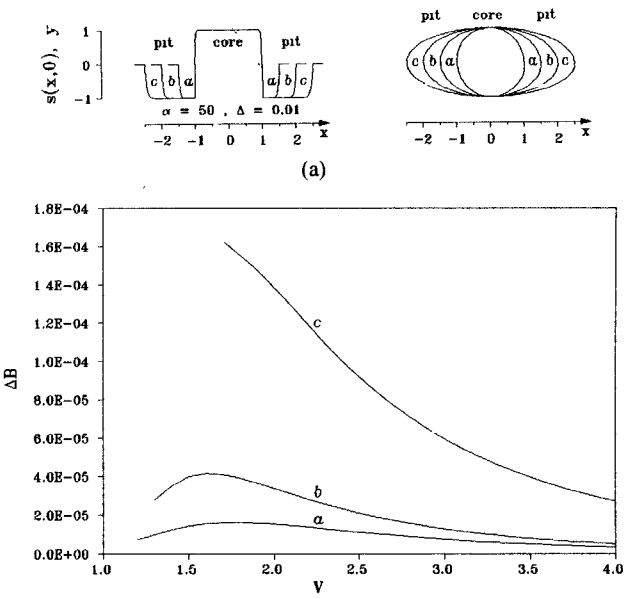

Fig. 7. Canonical side pit structure. (a) Specification of the waveguide. (b) Modal birefringence ΔB of the HE_{11}^x and HE_{11}^y modes for different core to side pit proportions. Curves a, b, c correspond to the cases: $I_s > 0$, $I_s = 0$, $I_s < 0$, respectively.

(with Δ_g up to -30Δ) in example discussed above in subsection C (c.f. Fig. 6(a)).

In general, the performance of the IEEM strongly depends on the accuracy with which the eigenfield is evaluated in the successive iterations. Thus, use of an accurate integration procedure is a crucial prerequisite for obtaining high efficiency in more complicated cases.

The effectiveness of the IEEM can be expressed in terms of the ν and μ numbers introduced earlier, and the ι number N_ι, defined as the average (for a given plot) number of iterations producing $\Delta Z = |Z_n - Z_{n-1}|$ smaller than 10^{-5}. In the examples presented, these numbers were $N_\nu = 20$, $N_\mu = 45$, $N_\iota = (16$ and $8)$ for the A_1 mode of the structure with no rectangular symmetry (example in subsection B, Figs. 4 and 5), $N_\nu = 10$, $N_\mu = 45$, $N_\iota = 7$ for the example in subsection C, and $N_\nu = 10$, $N_\mu = 45$, $N_\iota = 9$ for the HE_{11}^x mode in case c of the example discussed in subsection D.

IV. Conclusions

The IEEM has proved its applicability to a wide class of dielectric structures including multicore waveguides and those with one symmetry axis only. To the best knowledge of the authors, results presented in the examples discussed in subsections III-B and III-C are new. The method appeared to be especially effective in finding the fundamental modes of a structure. Further modes can also be obtained, provided they are $\mathscr{H}$ orthogonal to the ones previously found and the initial approximation is properly chosen. Comparison with many recently published results confirmed the high accuracy and versatility of the method. Its capability of analyzing structures with complex valued profiles is encouraging with respect to further applications.

ACKNOWLEDGMENT

The authors wish to acknowledge the encouragement and support of Prof. E. Danicki, the Head of the Department. They also wish to thank Prof. J. Maczynski and Prof. P. M. van den Berg for their helpful comments during the completion of the manuscript.

REFERENCES

[1] C. Yeh, S. B. Dong, and W. Oliver, "Arbitrarily shaped inhomogeneous optical fiber of integrated optical waveguides," *J. Appl. Phys.*, vol. 46, pp. 2125–2129, May 1975.

[2] C. Yeh, K. Ha, S. B. Dong, and W. P. Brown, "Single-mode optical waveguides," *Appl. Opt.*, vol. 18, pp. 1490–1504, May 1979.

[3] K. Oyamada and T. Okoshi, "Two-dimensional finite-element method calculation of propagation characteristic of axially nonsymmetrical optical fibers," *Radio Sci.*, vol. 17, pp. 109–116, 1982.

[4] C. C. Su, "A combined method for dielectric waveguides using the finite-element technique and the surface integral equations method," *IEEE Trans. Microwave Theory Tech.*, vol. MTT-34, pp. 1140–1146, Nov. 1986.

[5] E. Schweig and W. B. Bridges, "Computer analysis of dielectric waveguides: A finite difference method," *IEEE Trans. Microwave Theory Tech.*, vol. MTT-32, pp. 531–541, May 1984.

[6] K. Bierwirth, N. Shultz, and F. Arndt, "Finite-difference analysis of rectangular dielectric waveguide structures," *IEEE Trans. Microwave Theory Tech.*, vol. MTT-34, pp. 1104–1113, Nov. 1986.

[7] J. M. van Splunter, H. Blok, N. H. G. Baken, and M. F. Dane, "Computational analysis of propagation properties of integrated-optical waveguides using a domain integral equation," in *Proc. URSI Int. Symp. E. M. Theory* part A, 1986, pp. 321–323.

[8] V. V. Shevchenko, "Alteration formula methods in the theory of dielectric waveguides and optical fibers," (in Russian), *Radiotkh. Eleckron.*, vol. XXXI, pp. 849–864, May 1986.

[9] E. F. Kuester, "The effective cross-section method for dielectric waveguides in or on a substrate," *Radio Sci.*, vol. 19, pp. 1239–1244, Oct. 1984.

[10] T. F. Jablonski, "Iterative eigenfunction expansion method for monomode gradient index fibers with arbitrary cross-sections," in *Proc. URSI Int. Symp. E. M. Theory*, part B, 1986, pp. 415–417.

[11] M. Reed and B. Simon, *Methods of Modern Mathematical Physics*, vol. 4. New York: Academic Press, 1978.

[12] T. F. Jablonski, "Iterative eigenfunction expansion method for cylindrical fibers" (in Polish), *IFTR Reports*, 3/1986.

[13] T. F. B. Jablonski and M. J. A. Sowinski, "Propagation properties of doublecore optical fibers," *SPIE* vol. 670, Optical Fibers and Their Applications IV (1986), pp. 30–38.

[14] C. C. Su and C. H. Chen, "Calculation of propagation constants and cutoff frequencies of radially inhomogeneous optical fibers," *IEEE Trans. Microwave Theory Tech.*, vol. MTT-34, pp. 328–332, Mar. 1986.

[15] K. Kitayama and Y. Ishida, "Wavelength-selective coupling of two-core optical fiber: application and design," *J. Opt. Soc. Amer.* A, vol. 2, pp. 90–94, Jan. 1985.

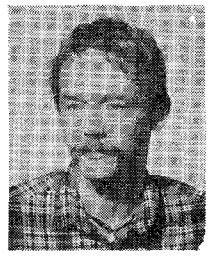

Tomasz Jabłoński was born in Bytom, Poland, on January 21, 1954. He received the M.Sc. degree in mathematical physics with first class honors from the University of Warsaw, Warsaw, Poland in 1978.

From 1978 to 1981 he was an assistant at the University of Warsaw, where he investigated problems in the spectral theory of operators. From 1981 to 1983, in the Institute of Telecommunication, Warsaw, he worked on applications of the antenna arrays theory. In 1984 he joined the Department of Electromagnetic Waves Theory of the Institute of Fundamental Technological Research, Warsaw. He is currently completing his Ph.D. degree on applications of the spectral theory of operators for solving electromagnetic boundary problems. At present, he is working on mathematical modeling of propagation in dielectric guiding structures.

Mr. Jabłoński is a member of the Association of Polish Electronic Engineers.

Maciej J. Sowiński was born in Warsaw, Poland, on July 24, 1947. He received the M.S. degree with first class honors in mathematics from the Warsaw University of Technology in 1971. In 1972 he joined the Department of Electromagnetic Waves Theory, Institute of Fundamental Technological Research, Warsaw, Poland, where he received the Ph.D. degree in 1980 and is now an Assistant Professor.

He has been engaged in research on guiding by metallic waveguides and microwave devices, dielectric optical waveguides, and applications of the null-field method and the eigenfunction expansion method to field problems. From 1987 to 1988 he was a research fellow in the Laboratory of Electromagnetic Research, Delft University of Technology, Delft, The Netherlands.

Dr. Sowiński is a member of the Association of Polish Electronic Engineers.